Pronounced Airy structure in elastic $^{16}O+^{12}C$ scattering at $E_{lab}=132$ MeV

A. A. Ogloblin,[1] Dao T. Khoa,[2] Y. Kondō,[3,4] Yu. A. Glukhov,[1] A. S. Dem'yanova,[1] M. V. Rozhkov,[1] G. R. Satchler,[5,6] and S. A. Goncharov[7]

[1]*RRC Kurchatov Institute, 123182 Moscow, Russia*

[2]*Department of Physics, Chung Yuan Christian University, Chung Li, Taiwan 32023, Republic of China*

[3]*Department of Natural Sciences, Kyoto Women's University, 35 Kitahiyoshi-cho, Imakumano, Higashiyama-ku, Kyoto 605, Japan*

[4]*Department of Theoretical Physics, RSPhysSE, The Australian National University, Canberra, ACT 0200, Australia*

[5]*Physics Division, Oak Ridge National Laboratory, Oak Ridge, Tennessee 37831-6373*

[6]*Department of Physics & Astronomy, University of Tennessee, Knoxville, Tennessee 37996*

[7]*Nuclear Physics Institute, Moscow State University, Moscow, Russia*

(Received 24 November 1997)

Measurement of elastic $^{16}O+^{12}C$ scattering at $E_{lab}=132$ MeV has been performed over the angular range $6°<\Theta_{c.m.}<125°$, which covers both the diffractive and refractive regions. A prominent minimum has been observed at $\Theta_{c.m.}\approx 86°$, which can be identified as an Airy minimum preceding the rainbow maximum. It thus provides the first clear experimental evidence for the refractive (rainbow) scattering pattern in the $^{16}O+^{12}C$ system. This Airy structure can be well described by discrete sets of optical potentials with a relatively weak absorption and a deep real potential. Candidates for the realistic family of $^{16}O+^{12}C$ optical potentials at $E_{lab}=132$ MeV are discussed; those include the semimicroscopic potential given by the double-folding model. [S0556-2813(98)05304-7]

PACS number(s): 25.70.Bc, 24.10.Ht, 21.30.Fe

In recent years, our knowledge of the interaction between heavy ions (HI's) has been broadened significantly, especially through studies of the elastic scattering of certain combinations of light heavy ions, for which the absorption is relatively weak and refractive effects appear. Refractive (rainbow) phenomena in nuclear scattering provide a unique source of information on the HI interaction potential at small internuclear distances (see, e.g., Refs. [1,2]). In particular, high-precision refractive scattering data have been used in folding analyses [3,4] to place constraints upon the value of the incompressibility of cold nuclear matter. So far, systematic experimental evidence of a nuclear rainbow in light HI scattering has been found mainly in two symmetric systems $^{12}C+^{12}C$ and $^{16}O+^{16}O$, with the most spectacular Airy pattern exhibited in elastic $^{16}O+^{16}O$ scattering at $E_{lab}=350$ MeV [5]. We note that elastic $^{16}O+^{16}O$ scattering data have been measured with extremely high accuracy at different energies [6] and show clearly the evolution of the refractive pattern in this system, which is very helpful for the study of the energy dependence of the HI optical potential.

While these two systems are quite ''transparent'' for refractive effects to appear, the Mott interference caused by the boson symmetry between the two identical nuclei sometimes leads to rapidly oscillating elastic cross sections at angles around $\Theta_{c.m.}=90°$, which in turn obscure Airy structures in this angular region. The whole Airy pattern might only be seen in an optical model (OM) calculation which removes the symmetrization artificially [7,8]. The $^{16}O+^{12}C$ system does not have boson symmetry, and has been suggested as a good candidate for the study of the nuclear rainbow [9]. However, available data for the $^{16}O+^{12}C$ system usually *do not* cover the refractive region in the angular distribution, and therefore are of little help in revealing the rainbow structure. We note that only two data sets for the $^{16}O+^{12}C$ system, at $E_{lab}=608$ MeV [10] and 1503 MeV [11], have been shown to contain some refractive features which are sensitive to the shape of real optical potential at small radii. However, the data at the former energy do not extend to sufficiently large angles to identify the Airy pattern [12], while the latter energy is too high to observe the ''rainbow'' unambiguously, since the refractive part of the angular distribution has moved forward and mixed with the diffractive part at forward angles. The present article reports on a new measurement of elastic $^{16}O+^{12}C$ scattering at $E_{lab}=132$ MeV, which was aimed to cover large scattering angles to find possible rainbow features.

The measurement has been performed at the Kurchatov Institute Cyclotron, where two experimental setups were used. The first one has been used to measure scattering events in the angular range $6°<\Theta_{c.m.}<102°$. It contained a E-ΔE telescope of semiconductor detectors. The thicknesses of the E and ΔE counters were 300 μm and 13 μm, respectively. The solid angle to the target was 0.08 msr. The target was a self-supporting carbon foil of 2.15 mg/cm^2 thickness. The average beam energy in the target was 132.3 MeV, with the energy resolution of the detector system about 1.5 MeV (determined mainly by kinematics). The angular resolution was $\pm 0.3°$ in the laboratory system and was determined mainly by multiple scattering on the target. Since the data at forward angles are needed with high precision to determine the absolute normalization of the data, this setup has been used in two separate runs for repeated measurement of scattering events at forward angles ($\Theta_{c.m.}<40°$).

As for the second setup, scattering events in the backward angles ($102°<\Theta_{c.m.}<125°$) have been measured with kinematic coincidences. Two detectors with a diameter of 25 mm were located on either side of the beam at distances of 200 mm and 150 mm from the target. For this setup, a carbon foil of 0.24 mg/cm^2 thickness was used for the target. The average beam energy was 132.2 MeV, and the angular resolution

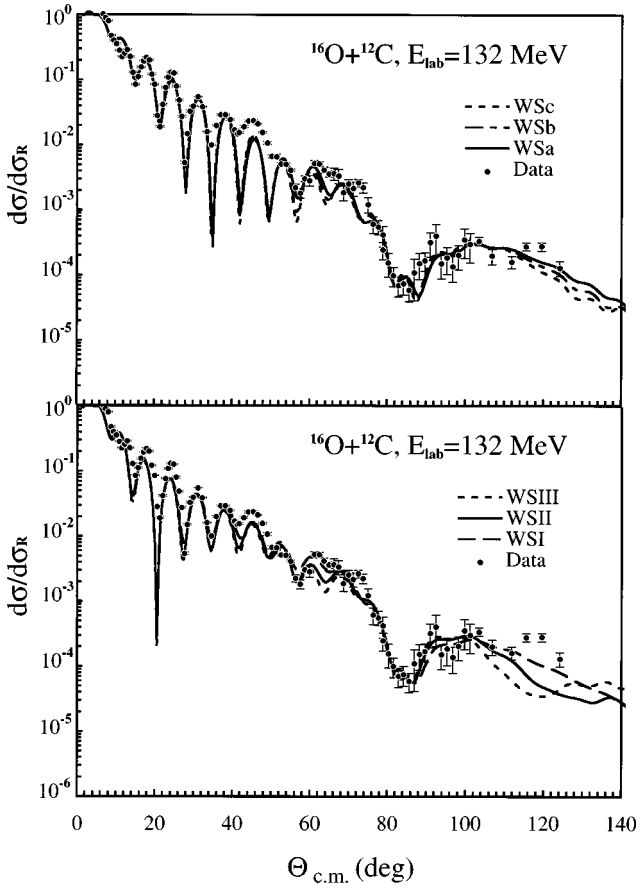

FIG. 1. Measured elastic $^{16}O+^{12}C$ scattering data at $E_{lab}=132$ MeV in comparison with OM fits given by two families of optical potentials of Woods-Saxon shape (see Table I).

was $\pm 0.3°$, which was determined mainly by the beam angular spread. Selected events were recorded event by event and treated off line. The absolute accuracy for the measurement was around 10%.

The measured angular distribution together with the OM fits given by different Woods-Saxon (WS) potentials is shown in Fig. 1. One can see that Fraunhofer diffractive oscillations dominate up to about $\Theta_{c.m.}\approx 40°$, and are then followed by a ''modulating'' pattern in the transitional region ($\Theta_{c.m.}\approx 40°-60°$). The fall to a minimum at about 86° and the rise afterwards belong clearly to the refractive part of the elastic cross section.

In the OM analysis of the present data, we have tried both the conventional six-parameter WS form factor and that raised to the power of 2. These two choices lead to about the same optical potential families which fit the data equally well. For simplicity, we present hereafter the results obtained with the standard WS form factor. Thus the $^{16}O+^{12}C$ optical potential in our OM analysis is as follows:

$$U(R)=V_C(R)-V\left[1+\exp\left(\frac{R-R_V}{a_V}\right)\right]^{-1} - iW\left[1+\exp\left(\frac{R-R_W}{a_W}\right)\right]^{-1}, \quad (1)$$

and the WS parameters were adjusted to obtain the least χ^2 fit to the scattering data, assuming a 10% uncertainty for all data points in order to obtain a better reproduction of the data at large angles.

A folding analysis has also been performed. In this case, the real optical potential $V_F(R)$ is calculated within an ''extended'' version of the double-folding model [13], using the newly parametrized (BDM3Y1) density-dependent version of the so-called M3Y interaction based on the G-matrix elements of the Paris NN potential (see details in Refs. [3,4]). The nuclear densities used in the folding-model calculations are taken as Fermi distributions with parameters [14] chosen to reproduce the shell-model densities for ^{16}O and ^{12}C and which give the rms charge radii deduced from electron scattering. The optical potential in such a folding analysis is

$$U(R)=V_C(R)+N_R V_F(R)-iW\left[1+\exp\left(\frac{R-R_W}{a_W}\right)\right]^{-1}, \quad (2)$$

where the renormalization factor N_R together with the parameters of the imaginary potential was adjusted to fit the data. The Coulomb potential $V_C(R)$ used in both the folding calculation and the OM analyses is generated by folding two uniform charge distributions, with radii taken from the electron scattering data for the considered nuclei (3.54 fm for ^{16}O and 3.17 fm for ^{12}C). All the OM analyses were made using the nonrelativistic code PTOLEMY [15].

Our six-parameter OM search resulted in several local χ^2 minima; corresponding to these, two families of discrete WS sets (WSa, WSb, WSc and WSI, WSII, WSIII) are listed in Table I. While the imaginary WS potentials are more or less of the same strength, the obtained real WS potentials have different depths which result in different volume integrals per interacting nucleon pair J_V. In the tail region they all have about the same strength to reproduce the Fraunhofer diffraction correctly. Theoretical descriptions of the elastic data given by the three sets of WS potentials belonging to the first family (WSa, WSb, and WSc) are shown in the upper part of Fig. 1, and those given by the second family (WSI, WSII, and WSIII) are shown in the lower part. One can see that they all provide reasonable fits to the data, with a difference in the deepest minimum in the calculated cross sections. Potentials WSa, WSb, and WSc all produce the deepest minimum of the elastic cross section at $\Theta_{c.m.}\approx 35°$, while WSI, WSII, and WSIII potentials give the deepest minimum at around 21°. The first potential family describes better the forward part of the measured angular distribution, while the second family seems to reproduce better the medium angle part ($\Theta_{c.m.}\approx 40°-60°$), and hence they have comparable χ^2 values (see Table I). A more extensive data set at forward angles (like those measured for the $^{16}O+^{16}O$ system [5,6]) might well resolve the ambiguity in these two potential families. Despite this, as we will see below, the large angle structure of the cross section given by these two families of WS potentials has the same refractive origin.

One can see that the observed minimum at $\Theta_{c.m.}\approx 86°$ is reproduced quite well by all sets of the $^{16}O+^{12}C$ optical potential under study, with the following broad rainbow maximum slightly better described by the first potential family. This kind of (discrete) ambiguity in the real part of the optical potential is similar to that found in recent OM analy-

TABLE I. Optical potential parameters used in the OM analysis of the elastic $^{16}O+^{12}C$ data at $E_{lab}=132$ MeV [see Eqs. (1) and (2)]. χ^2 values are per datum, and were obtained with uniform 10% errors. A1, A2, A3, and A4 indicate the first-, second-, third-, and fourth-order Airy minima in the cross section at $\Theta_{c.m.}\approx 86°$.

Potential	V (MeV)	R_V (fm)	a_V (fm)	J_V (MeV fm^3)	W (MeV)	R_W (fm)	a_W (fm)	σ_{min} at $\Theta_{c.m.}\approx 86°$	σ_R (mb)	χ^2
WSa	173.6	4.01	0.72	322	18.3	5.76	0.58	A2	1474	16.1
WSb	223.9	3.93	0.69	387	20.2	5.72	0.58	A3	1486	16.8
WSc	281.0	3.83	0.68	451	21.9	5.68	0.59	A4	1493	17.8
WSI	182.1	3.38	0.96	275	16.7	5.82	0.56	A1	1483	14.8
WSII	260.5	3.12	0.93	327	18.4	5.82	0.55	A2	1498	16.8
WSIII	373.9	2.76	0.94	371	20.1	5.79	0.55	A3	1507	19.4
Folding	0.88 [a]	—	—	310	18.6	5.83	0.56	A2	1479	19.0
Folding [b]	0.88 [a]	—	—	309	16.6	5.83	0.56	A2	1460	7.4

[a]Renormalization coefficient N_R for the folding potential.
[b]Results of the folding analysis of the elastic $^{16}O+^{12}C$ data at $E_{lab}=139$ MeV. χ^2 values were obtained using the experimental errors.

ses of elastic $^{16}O+^{16}O$ scattering [7,8]. The microscopic potential given by the double-folding model [3,13] (renormalized by a factor $N_R=0.88$) is quite close to the WSII potential at small radii (see Fig. 2), and generates cross sections at large angles close to those given by the WSII potential (compare Figs. 1 and 3). For $R>6$ fm, the folding potential is significantly less attractive than the WSII potential, and as a result it generates elastic cross sections at forward angles somewhat closer to those given by the first family of WS potentials (compare the upper part of Fig. 3 with, e.g., the results given by the WSa potential in Fig. 1). We note that the real volume integral per interacting nucleon pair, J_V, equals 310 MeV fm^3 for the folding and 322 and 327 MeV fm^3 for the WSa and WSII potentials, respectively. These values agree quite well with the global systematics established in light HI scattering (see Fig. 2 in Ref. [17]). Since our version of the folding model [3,4] treats the energy dependence of the real HI optical potential quite accurately, we

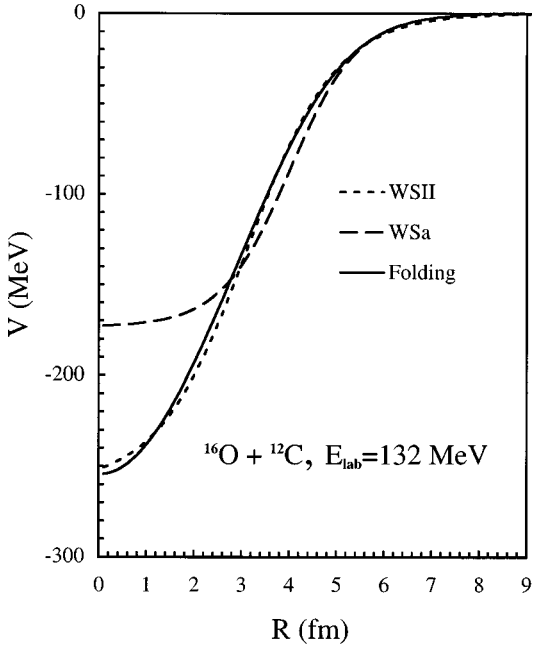

FIG. 2. Radial shape of WSII and WSa (real) optical potentials for the $^{16}O+^{12}C$ system at $E_{lab}=132$ MeV in comparison with the folding (BDM3Y1) potential renormalized by a factor $N_R=0.88$. These three potentials reproduce the minimum in the elastic cross section at $\Theta_{c.m.}\approx 86°$ as the second-order Airy minimum (A2).

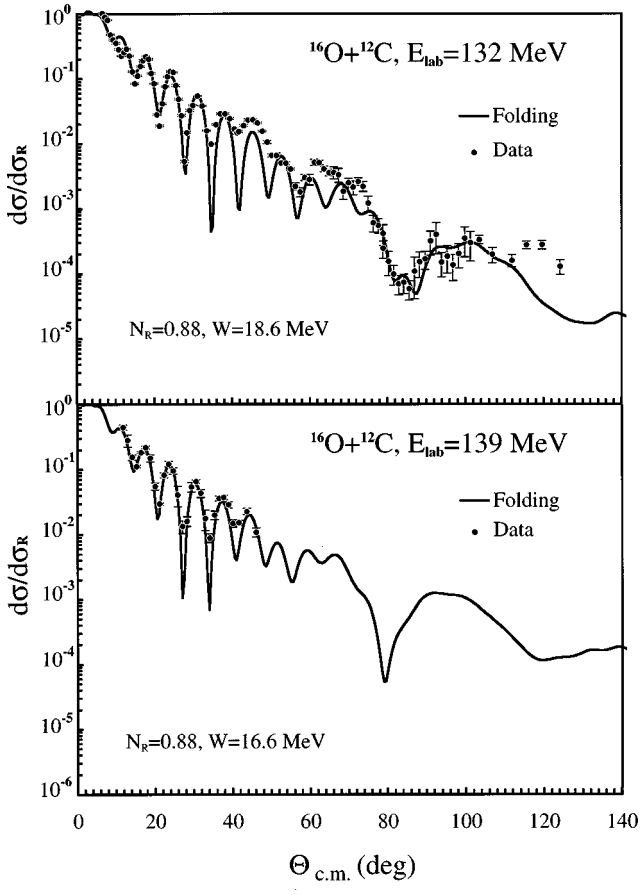

FIG. 3. Measured elastic $^{16}O+^{12}C$ scattering data at $E_{lab}=132$ and 139 MeV in comparison with the OM fits given by the real folding (BDM3Y1) potential and imaginary WS potential with depth $W=18.6$ and 16.6 MeV, respectively; other WS parameters were taken from Table I.

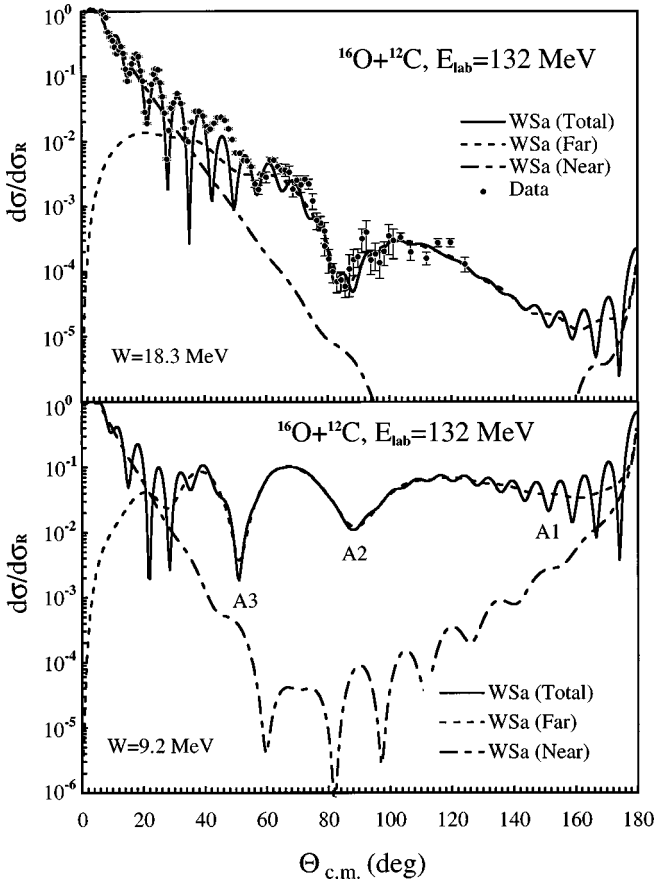

FIG. 4. Decomposition of the $^{16}O+^{12}C$ elastic scattering amplitude given by the WSa set of the optical potential into the near- and far-side components using Fuller's method [18]. The upper part shows OM results obtained with the potential parameters given in Table I; the lower part shows those obtained with a weaker absorptive imaginary potential ($W=9.2$ MeV; R_W and a_W were taken the same as those given in Table I). A1, A2, and A3 indicate the first-, second-, and third-order Airy minima in the far-side cross section, respectively.

expect that the folding potential would also give a good prediction for the elastic cross section at an energy near 132 MeV. The nearest available data in energy for the $^{16}O+^{12}C$ system are those at 139 MeV [16] which have only a few points covering the most forward angles (see lower part of Fig. 3). The folding potential calculated for this energy (renormalized by the same factor $N_R=0.88$) and a WS absorptive potential of slightly reduced strength and the same geometry as that obtained at 132 MeV give an excellent fit to the data and predict a similar refractive behavior of the elastic cross section at 139 MeV (which could have been observed in the measurement [16] if it had covered a wider angular range).

To confirm that the present data at large angles are strongly refractive, we have also performed the decomposition of the elastic scattering amplitude into near- and far-side components, using the technique suggested by Fuller [18]. Results given by all versions of the optical potential under study (see, e.g., results given by the WSa potential plotted in the upper part of Fig. 4) allow us to conclude unambiguously that these $^{16}O+^{12}C$ data exhibit a clear refractive pattern, which is due to the dominance of the far-side scattering amplitude at large angles. The observed dip at $\Theta_{c.m.}\approx 86°$ is entirely due to a minimum in the cross section given by the far-side scattering amplitude, and can be interpreted as an Airy minimum [17,19]. The question now is which of the Airy structures, given by different sets of the optical potential, is the most ''realistic'' and consistent with the results obtained for the neighboring $^{12}C+^{12}C$ and $^{16}O+^{16}O$ systems [7,8,19].

We note that a very detailed study of the energy dependence of the refractive pattern in elastic $^{12}C+^{12}C$ scattering has been made by McVoy and Brandan [19], where they showed unambiguously that the prominent minimum in the $\Theta_{c.m.}=90°$ excitation function at $E_{lab}=102$ MeV ($E_{c.m.}=51$ MeV) is due to the second Airy minimum crossing 90° at that particular energy. We have made an analogous estimation for the $^{16}O+^{12}C$ system, using different sets of the optical potentials given in Table I. The Airy structure is easily revealed in the OM calculation with a given set of the optical potential, by gradually increasing the incident energy until the first Airy minimum and the primary rainbow (with its broad exponential falloff tail) are clearly seen. For the WSa and WSII potentials, the 90° second Airy minimum (A2) appears at $E_{c.m.}=54.8$ and 54.0 MeV, while for the WSb and WSIII potentials the 90° dip appears at $E_{c.m.}=55.0$ and 53.8 MeV, but they correspond to the third Airy minimum (A3). With the beam energy of the present measurement slightly larger than those used in these estimations ($E_{c.m.}\approx 56.6$ MeV), this Airy minimum is naturally shifted into smaller angles and has been indeed observed in the experiment. In general, we can show that the observed minimum at $\Theta_{c.m.}\approx 85.6°$ in the measured angular distribution can be described as the first- (A1), second- (A2), and third- (A3) order Airy minima by WSI, WSII, and WSIII sets of the optical potential and as the second- (A2), third- (A3), and fourth- (A4) order Airy minima by the WSa, WSb, and WSc sets, respectively. The best-fit folding potential is quite close in shape to the WSII real potential at small distances and also describes this minimum as A2.

It is well known that the Airy structure in the refractive part of the angular distribution is built up by an interference between the $l_<$ and $l_>$ components of the far-side amplitude [1,2,19] which correspond to the trajectories at smaller and larger impact parameter, respectively. Since the $l_<$ subamplitude of the far-side scattering is usually suppressed by absorption in the considered $^{16}O+^{12}C$ system, the Airy oscillating pattern in turn is also obscured by the absorptive imaginary potential. In order to better illustrate the Airy pattern of the new data, we have performed the OM calculation and the near-far decomposition of the scattering amplitude given by the WSa potential, where the strength of the imaginary WS potential (see Table I) was reduced by about 50%. These results are plotted in the lower part of Fig. 4, with the Airy minima from the first to the third order are all visible in the angular region (indicated as A1, A2, and A3). One finds that the A2 minimum (corresponding to the one observed in experiment around 86°) remains almost at the same angle, while the structure and location of the other Airy minima are strongly affected by the absorption. We note that about the same picture can be obtained for the WSII potential, while for the WSb or WSIII potential the A1 minimum remains

beyond 180° (in the dark side of the rainbow) and only A2, A3, and A4 are visible (with A3 located around 86°).

Although the present data seem to be not sufficient for us to make an unambiguous conclusion about the order of the observed Airy minimum at around 86°, a *tentative* guess can be made based on previous studies of the Airy structure in the neighboring $^{12}C+^{12}C$ and $^{16}O+^{16}O$ systems [7,8,19]. Usually dominance of the *primary* rainbow occurs when the incident energy is up to about 20–25 MeV/nucleon [1,2], with the measured $^{16}O+^{16}O$ elastic scattering at $E_{lab}=350$ MeV [5] as a typical example. If this is really a universal rule, the WSI potential is *not* the right candidate for the $^{16}O+^{12}C$ optical potential at the energy of the present measurement (8.25 MeV/nucleon). The WSI potential also has the real volume integral per nucleon pair (J_V) equal to 275 MeV fm^3, which deviates significantly from the global trend observed in light HI scattering [17], where J_V is expected in the range 310–370 MeV fm^3 at this energy. In addition, results obtained from a consistent OM description of the elastic scattering angular distributions and the 90° excitation function for the $^{16}O+^{16}O$ system [8] suggest that $J_V \approx 337$ and 329 MeV fm^3 at ^{16}O incident energies of 124 and 145 MeV, respectively. These considerations suggest that realistic families for the $^{16}O+^{12}C$ optical potential at $E_{lab}=132$ MeV are perhaps those presented by WSa and WSII potentials, which give the J_V values within the expected range. The WSa and WSII potentials also reproduce the same order of Airy minimum as given by the microscopic folding potential. We note that the WSII potential is also closer to an extrapolation of the recent OM results for the $^{16}O+^{12}C$ scattering data at lower energies and the low-energy resonances found for this system [20].

Finally we note that the last three data points seem to indicate some enhancement of the cross section at $110° < \Theta_{c.m.} < 125°$, which cannot be described, e.g., by the folding potential (see upper part of Fig. 3). The folding model potential can be represented as the first-order term of the formal optical potential given by Feshbach's reaction theory [21]. This potential is defined, when used in the one-body Schrödinger equation, to generate the relative motion part of the total wave function of the HI system in which the two colliding nuclei remain in their ground states. In this sense, the folding potential does not contain explicitly contributions from the coupling to the nonelastic channels, which is usually referred to as the ''dynamic polarization potential'' (DPP). In the present case, the enhancement in the last data points might well be due to the elastic ($Q=0$) alpha transfer process $^{12}C(^{16}O,^{12}C)^{16}O$, which could give rise to the measured (elastic) cross section at backward angles [22]. Such a process could give a sizable contribution to the real part of the DPP which could change the shape of the folding potential. In principle these effects would be included in a full coupled reaction channel (CRC) calculation [23]. In practice, one usually adopts a renormalization procedure in the folding model or assumes a more flexible form for the real optical potential that could account effectively for the contributions from the DPP. We note that preliminary results of the CRC calculation [24] for elastic alpha transfer in the $^{16}O+^{12}C$ system at 132 MeV obtained with the WSII potential (which is very close in shape to the folding potential) show that the elastic alpha transfer can indeed enhance elastic cross sections at large angles, although the effect still depends strongly on the parameters used to calculate the wave function of the alpha particle bound in the ^{16}O nucleus and the spectroscopic factors assumed. This interesting aspect needs (and deserves) a separate and more extensive study, including measurements on the ^{12}C produced at forward angles.

In summary, the elastic $^{16}O+^{12}C$ scattering data at $E_{lab}=132$ MeV have been measured over a wide angular range and analyzed within the standard optical model. The observed dip at $\Theta_{c.m.} \approx 86°$ was shown to be an Airy minimum, probably of the second order. Such a scenario is also described by a semimicroscopic version of the optical potential, with its real part given by the double-folding model. Our OM analysis of the present data has confirmed that the $^{16}O+^{12}C$ system is a very suitable projectile-target combination for the experimental study of refractive (rainbow) phenomena in light HI scattering, and extensive measurements at higher energies are in progress in order to have a complete picture of the evolution of the Airy structure, like that found earlier in the $^{12}C+^{12}C$ and $^{16}O+^{16}O$ systems [5–8,19]. In this connection, the $^{16}O+^{12}C$ elastic angular distribution has the advantage of not being affected by the Mott interference (required for the two symmetric $^{12}C+^{12}C$ and $^{16}O+^{16}O$ systems).

We thank Wolfram von Oertzen for his comments on the effects of elastic alpha transfer and making available to us some of the CRC results for the $^{16}O+^{12}C$ system. Help with the measurement by Vladislav Trzaska and V.V. Paramonov is also appreciated.

[1] M. E. Brandan *et al.*, Comments Nucl. Part. Phys. **22**, 77 (1996).
[2] M. E. Brandan and G. R. Satchler, Phys. Rep. **285**, 143 (1997).
[3] Dao T. Khoa and W. von Oertzen, Phys. Lett. B **342**, 6 (1995); Dao T. Khoa *et al.*, Phys. Rev. Lett. **74**, 34 (1995).
[4] Dao T. Khoa, G. R. Satchler, and W. von Oertzen, Phys. Rev. C **56**, 954 (1997).
[5] E. Stiliaris *et al.*, Phys. Lett. B **223**, 291 (1989).
[6] G. Bartnitzky *et al.*, Phys. Lett. B **365**, 23 (1996).
[7] Y. Sugiyama *et al.*, Phys. Lett. B **312**, 35 (1993).
[8] Y. Kondō *et al.*, Phys. Lett. B **365**, 17 (1996).
[9] M. E. Brandan and G. R. Satchler, Phys. Lett. B **256**, 311 (1991).
[10] M. E. Brandan *et al.*, Phys. Rev. C **34**, 1484 (1986).
[11] P. Roussel *et al.*, Phys. Rev. Lett. **54**, 1779 (1985).
[12] G. R. Satchler, Nucl. Phys. **A574**, 575 (1994).
[13] Dao T. Khoa, W. von Oertzen, and H. G. Bohlen, Phys. Rev. C **49**, 1652 (1994).
[14] M. E. Farid and G. R. Satchler, Nucl. Phys. **A438**, 525 (1985).
[15] M. H. Macfarlane and S.C. Pieper, Argonne National Labora-

tory Report No. ANL-76-11, 1978; M. Rhoades-Brown, M. H. Macfarlane, and S. C. Pieper, Phys. Rev. C **21**, 2417 (1980); **21**, 2436 (1980).

[16] M. E. Brandan and A. Menchacha-Rocha, Phys. Rev. C **23**, 1272 (1981).

[17] M. E. Brandan and K. W. McVoy, Phys. Rev. C **55**, 1362 (1997).

[18] R. C. Fuller, Phys. Rev. C **12**, 1561 (1975).

[19] K. W. McVoy and M. E. Brandan, Nucl. Phys. **A542**, 295 (1992).

[20] C. Gao and Y. Kondō, Phys. Lett. B **408**, 7 (1997).

[21] H. Feshbach, *Theoretical Nuclear Physics* (Wiley, New York, 1992).

[22] W. von Oertzen and H. G. Bohlen, Phys. Rep., Phys. Lett. **19C**, 1 (1975).

[23] Y. Sakuragi, Phys. Rev. C **35**, 2161 (1987); Y. Sakuragi, M. Yahiro, and M. Kamimura, Prog. Theor. Phys. Suppl. **89**, 136 (1986).

[24] W. von Oertzen (private communication).